Universidad de Concepción
Dirección de Postgrado
Facultad de Ingeniería - Programa de Magíster en Ciencias de la Ingeniería con Mención en Ingeniería Civil

Evaluation of temperature effect on the dynamic parameters of a simply supported bridge: laboratory experiments and numerical models.

Evaluación del efecto de la temperatura en los parámetros dinámicos de un puente simplemente apoyado: experimentos de laboratorio y modelos numéricos.

Tesis para optar al grado de Magíster en Ciencias de la Ingeniería con mención en Ingeniería Civil

NICOLÁS ALFONSO GUZMÁN SOTO
CONCEPCIÓN-CHILE
2016

Profesor Guía: Fernando Cerda Carrizo
Dpto. de Ingeniería Civil, Facultad de Ingeniería
Universidad de Concepción

ABSTRACT

We are interested in the effect of freezing and non-freezing temperature distributions on the dynamic parameters of a simply supported bridge. A laboratory scale model is placed on a climate chamber, where a uniform variation of temperature from 0 to 40 °C is applied. Afterwards, a calibrated FEM model is used to simulate further freezing temperature scenarios.

Above the freezing point, results show an increase of temperature has a direct correlation on the decrease of fundamental frequency, with a maximum variation of 0.92%. Laboratory non-uniform temperature distribution, across the deck, only presents a slight variation in fundamental frequency, not considering it a crucial parameter to be studied.

Damage is also simulated on the finite elements model, where the variation of frequency caused by a severe damage scenario is within the same order of magnitude as the variation caused by uniform non-freezing temperature distribution. Furthermore, freezing temperature scenarios, generated on an enhanced finite elements model show a correlation between bending vibrational modes and soil stiffness variation due to temperature. Under freezing temperature scenarios, torsional vibrational modes are correlated with the variation of elasticity of the deck. Below the freezing point, frequency variation is up to twelve times higher than non-freezing results for simply supported configurations.

Finally, a simplified normalization method for data under temperature varying condition is proposed. For more complex structures, the evaluation of temperature effect should be addressed in order to avoid misdiagnosed bridge conditions through automated structural health monitoring systems (SHMS).

'¡Bendita perseverancia la del borrico de noria!

—Siempre al mismo paso. Siempre las mismas vueltas. —Un día y otro: todos iguales.

Sin eso, no habría madurez en los frutos, ni lozanía en el huerto, ni tendría aromas el jardín.'

Camino 998. San Josemaría Escrivá de Balaguer.

INDEX OF CONTENTS

INDEX OF TABLES

INDEX OF FIGURES

SECTION 1 INTRODUCTION

1.1 Research motivation

Chile has an estimated network of 12.000 bridges, which require a system of periodic assessment and analysis of their structural condition. The structural integrity of the Chilean bridges is not updated by a regular inspection or monitoring program and the condition of bridges involved in seismic events and the accumulated deterioration effect has not been studied in depth, having a greater risk of failure for future seismic events.

In the United States, according to the latest report of the American Society of Civil Engineers, about one of every ten bridges presents a structural condition that must be addressed in the near future. To solve this problem by 2030, the Federal Highway Administration estimates an investment of US$20.500 million needed per year, however, the current yearly budget is US$12.800 million. Therefore, it is required a continuous 'health' control system in structures, in order to reduce repairing costs and safeguard people's lives throughout time.

Current structural health monitoring systems involve the installation of sensors along a structure for different types of data acquisition, such as acceleration, strain, pressure, humidity and temperature, among many others. Data gathered by sensors is then processed and analyzed in order to get insights that would help experts on taking decisions about the health of the structure.

Two major obstacles for damage detection in structural health monitoring are the operational and environmental conditions on the dynamic response of structures, where changes produced by the latter could be within the same range as those produced by induced damage. Hence, for a proper assessment of the health condition of a structure it is required to study the effect of environmental conditions on the dynamic response of bridge structures, more importantly the effect of freezing temperature environments.

1.2 Hypothesis

Varying temperature scenarios generate stiffness changes in the surface deck and surrounding soil of a bridge, which can be identified and normalized from the extracted dynamic response of a bridge, allowing for improved damage detection and conditions diagnostics.

1.3 General objective

Identify and quantify the effect of low temperature on the response of bridge structures and extrapolate, using numerical models, the expected effect for several structural configurations.

1.4 Specific objectives

i. Design and build a laboratory setup for temperature testing of a simply supported bridge structure.

ii. Evaluate the effect of temperature on different structural bridge configurations, considering multiple deck elasticity and surrounding soils.

iii. Propose a simplified method to estimate frequency changes in bridges at low temperature scenarios.

iv. Propose a method to obtain normalization curves for bridge data, altered by temperature effects for future use in structural health monitoring prototype algorithms.

1.5 Methodology

This research is based on a simplified scaled bridge model located in the structures laboratory in the Civil Engineering Department of the University of Concepción (Guzmán, 2015). A finite element model is developed and calibrated to the scale to obtain results from the laboratory setup.

The model is further modified to incorporate springs on each support, to simulate the surrounding soil at different temperatures, including below the freezing point. Additionally, a layer material is added to the bridge deck, in order to simulate the effect of ballast or asphalt at freezing temperatures. Finally, frequency variation surfaces for the two first bending and torsional modes are generated. Several numerical simulations are preformed to observe variation patterns of vibration frequencies and mode shapes with respect to ambient temperature variations.

1.6 Results and conclusions

Results show a direct relationship between the layer material elasticity modulus and frequency response on each vibrational mode studied. Furthermore, in some scenarios, an increase of rigidity on simulated surrounding soil due to freezing has a greater influence on frequency than changes produced by deck elasticity variations, showing a frequency variation up to twelve times higher for a simply supported configuration. Variations of frequency in torsional modes are more related to surface deck changes due to temperature, where variations of frequency in bending vibrational modes are related to changes on simulated soil.

Previous research on the laboratory model, showed variations less than 1% in frequency, for global temperature changes from 0 °C to 40 °C, where simulated damage scenarios were in the order of 2% of variation. This study shows variation on the dynamic properties, due to freezing scenarios, could vary up to 12%, stressing the need for normalization methods in structural health monitoring to avoid misdiagnosis.

A structural health monitoring system should not only consider the structure itself but also the soil-structure interaction. Bridge structures located in freezing environments must consider a previous analysis of its behavior under low temperature scenarios, where high frequency changes could lead to alerts under normal operational conditions. This issue can be studied using a simplified analysis as proposed in this research.

1.7 Thesis organization

This thesis is organized as follows: Section 2 presents the theoretical framework, which introduces the reader into the state of the art of temperature effect on bridges. Section 3 includes a description of the developed laboratory model, numerical model and monitoring system used. Section 4 discusses tests results on the model and proposes a normalization method for data of bridges under temperature effects. Finally, Section 5 provides concluding remarks and future research lines.

SECTION 2 THEORETICAL FRAMEWORK

2.1 Introduction

In a Structural Health Monitoring System (SHMS), dynamic parameters, such as: natural frequencies, damping, and mode shapes; allow evaluating the structural condition of bridge structures. These systems have to take into account environmental and operational conditions to avoid false positives. As an example, temperature variations affect the dynamic response of a structure, being in some cases as significant as changes produced by low damage scenarios (Farrar, 1994). Nevertheless, dynamic behavior of structures under extreme environmental conditions, such as seasonal frost in cold zones, is still not understood completely.

This section describes the actual state of the art of dynamic analysis of bridge structures under low temperature scenarios. It is divided into two topics: temperature effect on bridges, and temperature effect on soil.

2.2 Temperature effect on bridges

Farrar *et al.* (1994) study the I-40 bridge over Rio Grande in New Mexico before it is demolished. Four progressive damage scenarios are induced to validate structural health monitoring procedures, as shown in Figure 2.1.

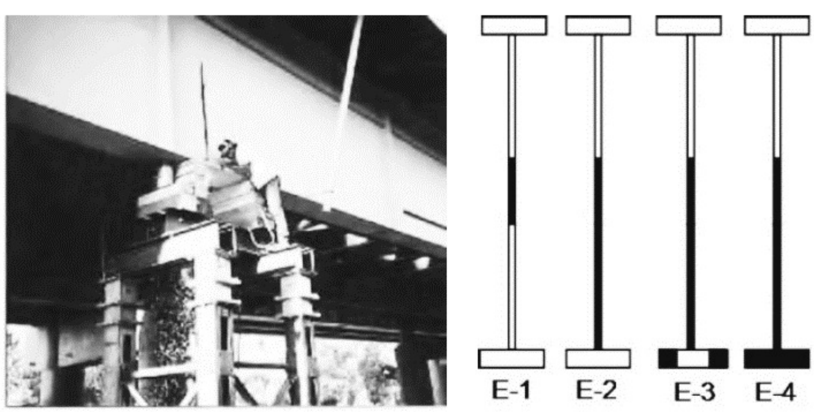

Figure 2.1 Four levels of incremental damage in beam of I-40 bridge (Farrar *et al.*, 1994).

Considering vibrational frequency of a bridge is proportional to flexural rigidity, it is expected fundamental frequency to decrease when damage increases. However, the first bending mode increases within the first and second damage scenario, decreasing with the third and fourth scenario (Figure 2.2). Further analyses indicate that, even though damage was present, temperature effect caused a major role in this variation.

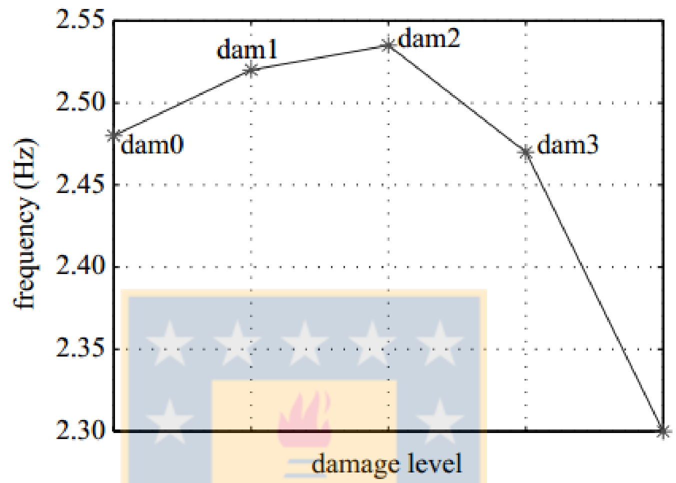

Figure 2.2 Variation in fundamental frequency across different damage scenarios (Sohn, 2007).

This research stresses how temperature variations could induce changes in dynamic properties within the same order of magnitude as the variation produced by damage. Further analysis is needed to understand the effect of temperature and its magnitude effect compared to damage scenarios.

Gonzalez *et al.* (2013) study the variation on the dynamic response of a railway bridge structure located in the city of Skidtrask, northern Sweden. This location has approximately a temperature differential of 60 degrees Celsius between the highest and lowest temperature records (Figure 2.3), with a minimum of -30 °C in the month of March during the five months of seasonal cold weather. As can be seen in Figure 2.4, below the freezing point, an increment on frequency is present, with a higher variation on the first torsional mode, achieving an increase on frequencies of 15% and 35% on the first bending mode and the first torsional mode correspondingly.

Frequency variation due to temperature changes above the freezing point is less than 5% for both vibrational modes.

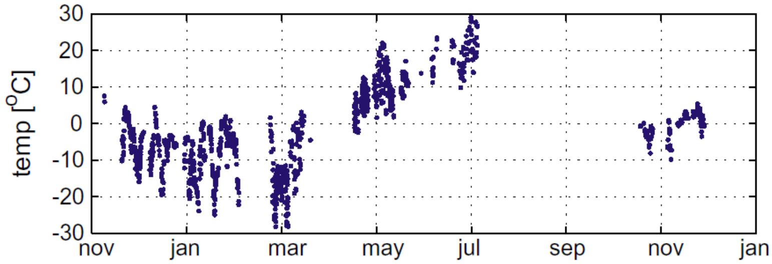

Figure 2.3 Temperature variation during monitoring period (Gonzalez *et al*., 2013).

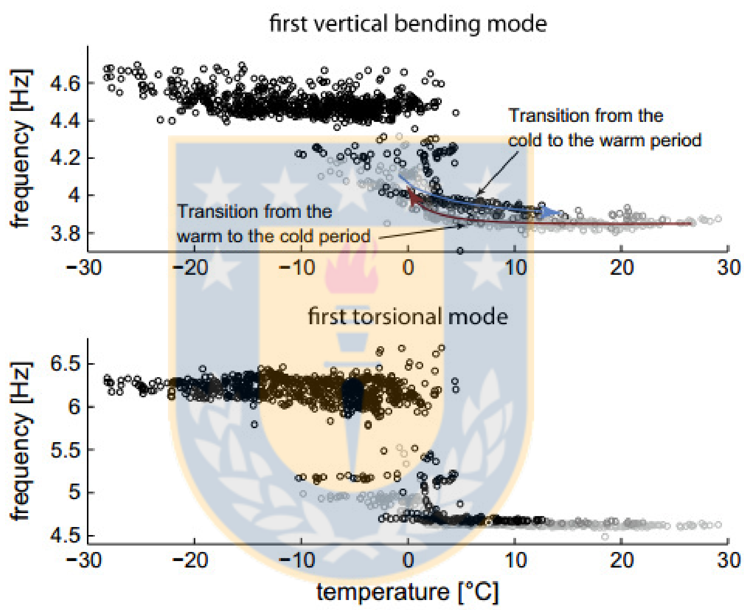

Figure 2.4 Frequency variation of first bending and first torsional mode of the Skidtrask railway bridge (Gonzalez *et al*., 2013).

A finite element model is created and analyzed with a Markov-Chain Monte Carlo updating. Authors attribute the frost in the ground and the formation of ice on the railway for explaining the dynamic behavior of the bridge. Due to the sensitivity found between the first bending mode and the soil stiffness and the first torsional mode and the ballast stiffness, authors explain a rapid defrosting of the ballast, related to its exposure to climate, leads to a higher frequency change. Further research of temperature effect on damping or modal shapes is not made.

Zabel *et al.* (2010) study a ballasted railway bridge in Central Germany, where temperature varies from -5 to over 20 °C approximately. The research finds an increase of the natural frequencies of the system under a temperature of 5 °C, with a maximum variation of 33% in the fourth vibrational mode, as shown in Figure 2.5.

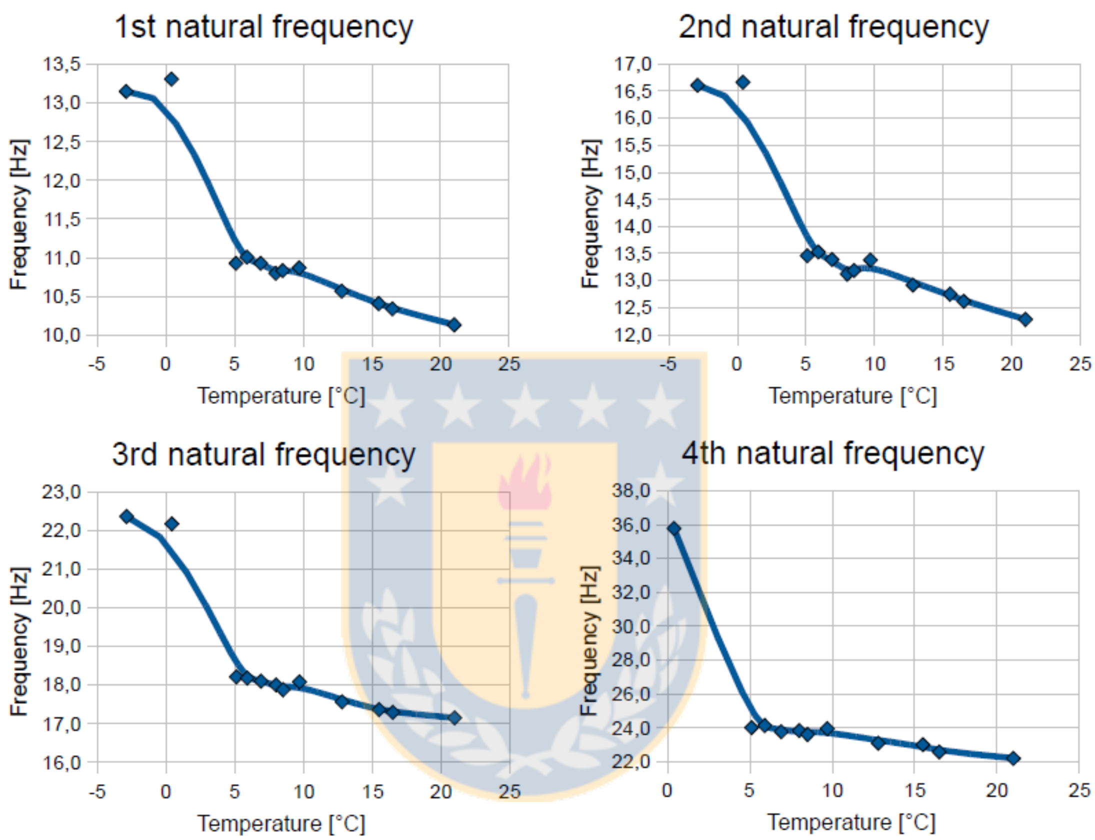

Figure 2.5 Identified bridge natural frequencies and air temperature (Zabel *et al*., 2010).

A finite element model is created to simulate and study the governing parameters of the system. With a sensitivity analysis, nine parameters are found to be governors of the system in frequency variation, those include: density of concrete and ballast, Young modulus of materials, supporting springs stiffness and shear modulus of bearings. After a 24-hour optimization, results show that two parameters have a strong dependency on the temperature variations: elasticity modulus of the bridge deck and shear modulus of the bearings (Figure 2.6), where the latter determine the stiffness of the springs at the supports. Nevertheless, authors state the initial upper and lower boundaries of the optimization may lower the results and not fully represent the behavior of the studied bridge.

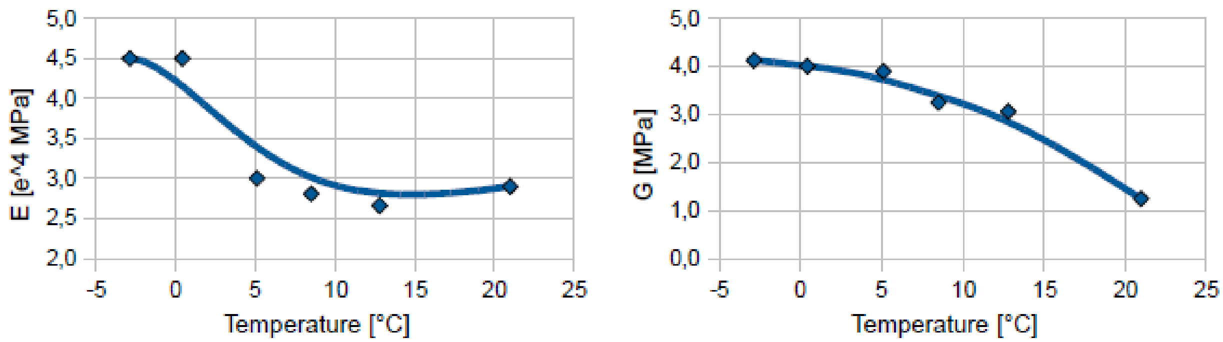

Figure 2.6 Optimization results for Young modulus of bridge deck (left) and shear modulus of bearings (right) (Zabel *et al*., 2010).

Peeters and De Roeck (2000) study the bridge Z24 located in Switzerland, for over a year, before it was artificially damaged. Figure 2.7 and Figure 2.8 show the frequency response for several deck temperature values, where a variation of frequency of 12% and 9% can be seen in the first and second natural frequency correspondingly. A bilinear curve is present for temperatures below zero degrees Celsius. Authors state this variation is closely related to the variation of temperature in the wearing surface, caused by changes in asphalt properties, and not due to the freezing of the soil around the boundaries of the bridge. Because linearity is assumed, low temperature data is disregarded in this study for further analyses. Finally, an ARX model is used to detect changes due to damage in the system considering temperature variations above the freezing point.

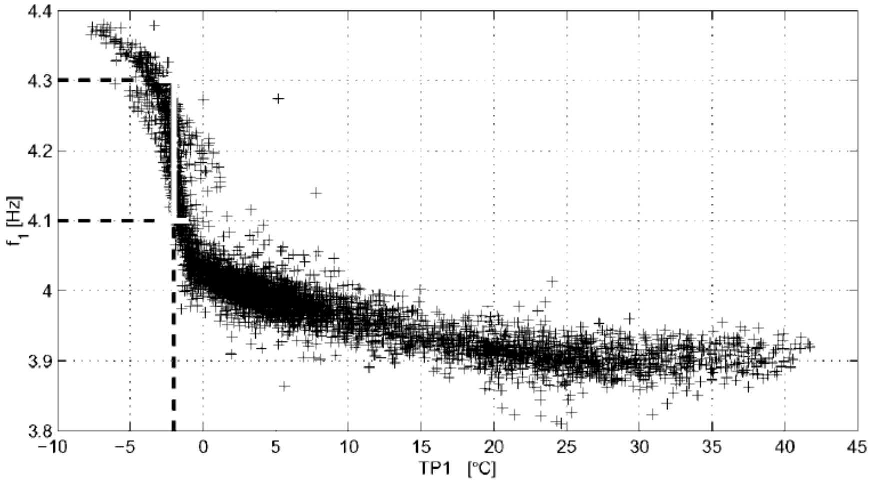

Figure 2.7 Z24 bridge fundamental frequency *vs* surface temperature (Peeters and De Roeck, 2001).

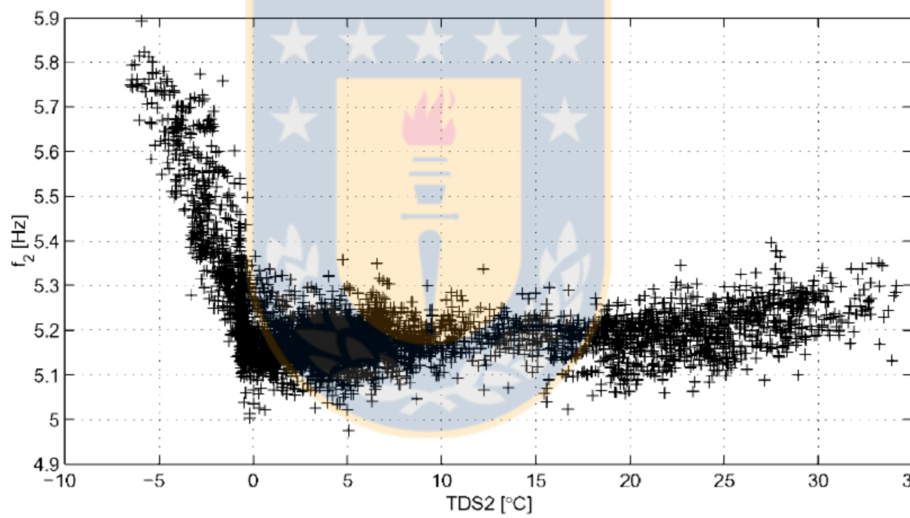

Figure 2.8 Z24 bridge second natural frequency *vs* deck soffit temperature (Peeters and De Roeck, 2001).

Yongda and DeWolf (2001) study the effect of temperature on a two-span bridge. The study shows how the natural frequencies of this bridge change during cold weather, having a frequency variation up to 21% in the second bending mode. Further analysis on the bearings show that freezing does not allow a free translation of the system, causing this behavior.

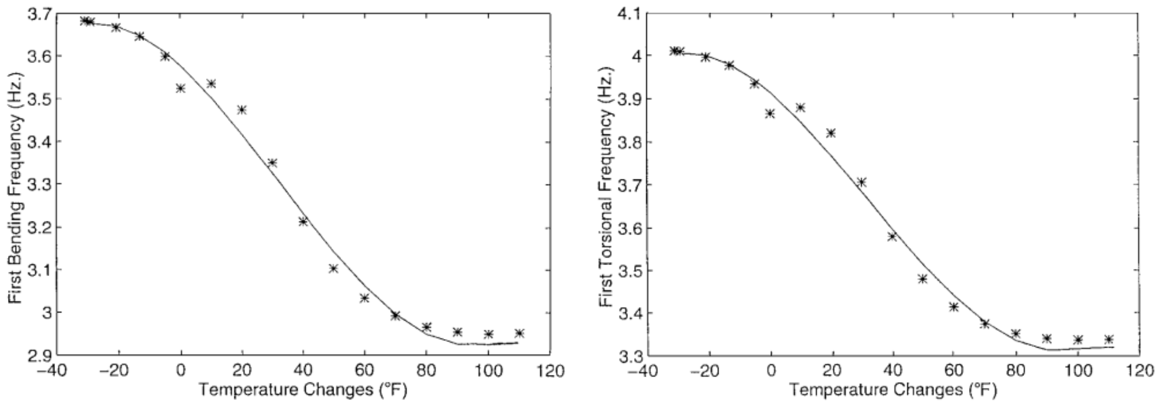

Figure 2.9 First bending and first torsional frequencies variation on finite element modelling compared with real data (Yongda and DeWolf, 2001).

A simplified finite element model is created to simulate and study the effect of freezing. Temperature effect is considered as restraining axial force along the model. Figure 2.9 shows how field data matches results from the finite element model. It is important to notice that the wearing surface or concrete slab performance under such low temperatures was not considered into analysis.

Temperatures below the freezing point may lead to variations in up to 30% on the dynamic properties of bridges, compared to the dynamic properties of bridges under thermal conditions above the freezing point. It is assumed this variation is caused mainly by changes in the surface deck and bearings restriction due to temperature. A study on the effect of soil under freezing temperature on the dynamic variation of bridges is also needed, which is addressed in this study.

2.3 Effect of temperature on soil

Simonsen *et al.* (2002) study the effect of seasonal frost conditions on the resilient properties of road materials for design methods. Coarse and fine-graded subgrade soils were tested from room temperature down to -10 °C and *vice versa*, in a freeze-thaw cycle. As can be seen in Figure 2.10, the resilient modulus of the subgrade soils tested show an increase under temperatures below 0 °C, having a variation in up to 2 or 3 times the order of magnitude.

In freeze-thaw cycles, all the soils decreased its resilient modulus from 20% to 60%, with a maximum increase in marine clay, as shown in Figure 2.11. The results presented by Simonsen *et al.* (2002) show the variability in elastic properties of soils and its importance in the study of soil-structure interaction monitoring.

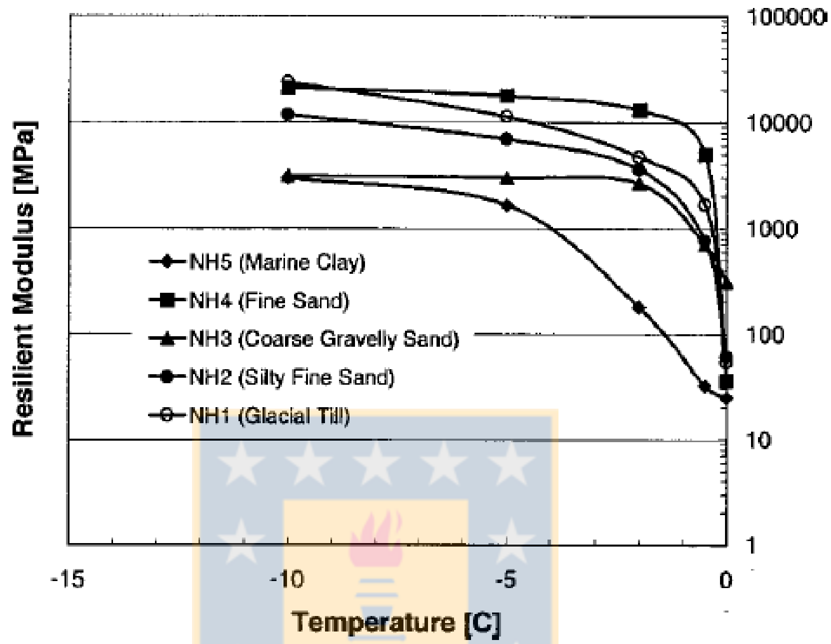

Figure 2.10 Resilient modulus of different soils as a function of temperature (Simonsen *et al.,* 2002).

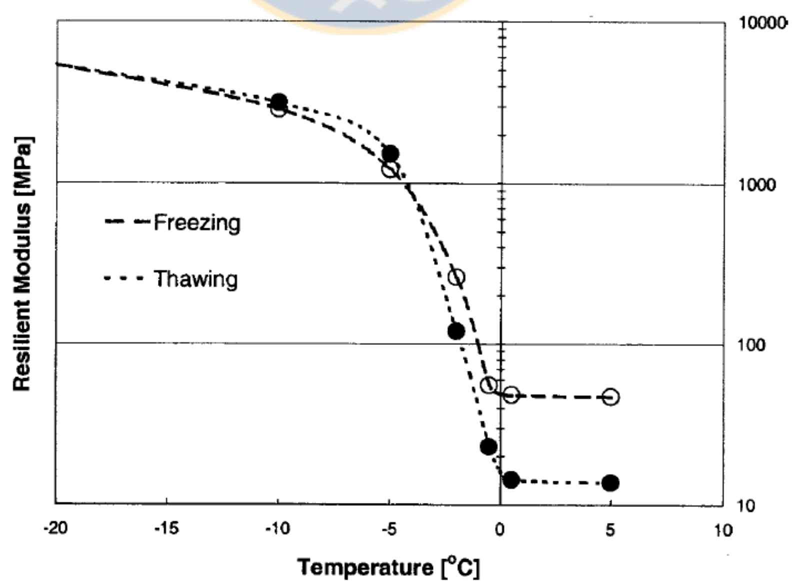

Figure 2.11 Resilient modulus and Freeze-Thaw effect on marine clay (Simonsen *et al.,* 2002).

Variations on mechanical properties of soils under different temperature scenarios, below the freezing point, show a similar behavior as the variations obtained in bridges under low temperature conditions. This might be an indicator on how the dynamic properties on bridges could be affected by the surrounding soil more than other variables.

2.4 Conclusions

Few studies are found on literature about the effect of freezing temperature on bridge structures, thus further research is needed to have a better understanding of the physical problem and the dynamic effects. Studies show variations up to 30% in frequency due to freezing temperatures. The magnitude of variations is in the same order of magnitude as severe damage scenarios. If not taken into account on bridge monitoring systems, severe damage could be undetected. Furthermore, freezing temperature effects on several soils studied show variations up to two times the order of magnitude on its elastic properties, having a similar behavior as the variation seen for temperature-induced frequency variation on bridges.

Most of the studies require long and time consuming optimizations based on on-site data. This is not practical for use in SHM systems where data normalization is required for real time monitoring. A more practical approach is needed and further developed within this study.

SECTION 3 LABORATORY AND FINITE ELEMENT MODEL DESCRIPTION

3.1 Introduction

This research focuses on the study of low temperature effect on a laboratory scaled bridge model. This model is located on the climate chamber of the Structures Laboratory in the Civil Engineering Department of the Universidad de Concepción.

This bridge model is instrumented with an accelerometer in the middle span, where acceleration data is used to obtain dynamic parameters of the structure, such as natural frequencies and damping. A FEM model, is then calibrated with laboratory data. The calibrated numerical model allows the creation and testing of multiple bridge and temperature scenarios for further analyses.

3.2 Model description

Guzmán (2015) evaluates the uniform and non-uniform temperature effect on an aluminum laboratory scaled bridge inside a climate chamber, from 0° to 40° C. The model is designed considering shifts in fundamental frequency as the main dynamic feature. The set-up is shown in Figure 3.1.

The model consists of a 3 x 0.55 m aluminum plate in top of two L shaped girders, where rivets and metal glue hold the parts together monolithically (Figure 3.1). The structure has a pinned and a roller support at each ending of the bridge (Figure 3.2). Each support has a nut and a threaded bolt for accurate vertical alignment. Both sides are mounted over concrete blocks (Figure 3.3).

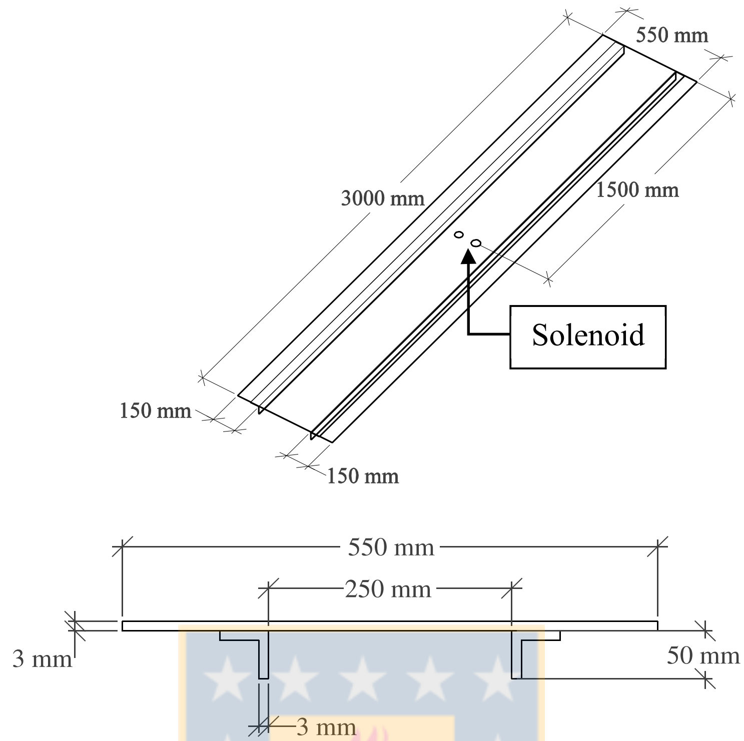

Figure 3.1 Dimensions of laboratory scaled bridge.

a) Pinned Support b) Rolller Support

Figure 3.2 Types of supports on laboratory model.

Figure 3.3 Laboratory scaled bridge model on climate chamber.

Two solenoids are used as the excitation source to induce free vibration motion of the bridge (Figure 3.4). The excitation source and the data acquisition system are integrated and controlled simultaneously by a computer outside the climate chamber.

The monitoring system consists of a ADXL 335 analog accelerometer, located at the bridge midspan, and a 16-bit NI-9205 National Instruments data acquisition module with programmable input ranges. For easy connection with the data acquisition module, the accelerometer is installed on a surface mount jack and connected through a RJ45 cable (Figure 3.5).

Sampling rate is set to 200 Hz. Fourier transform is used for identifying the natural frequencies, using only the fundamental frequency as the distinctive feature. Damping is identified by fitting an exponential envelope, and is validated with half power method.

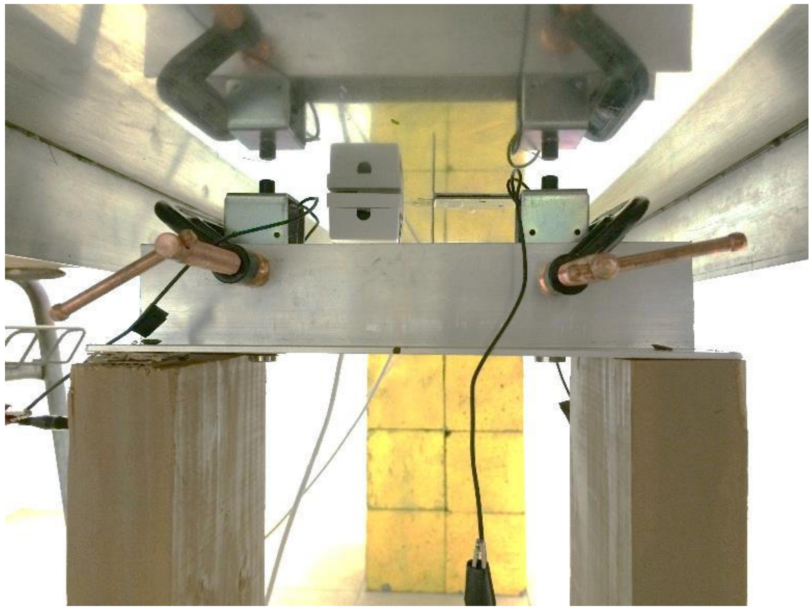

Figure 3.4 Solenoids excitation system at middle span.

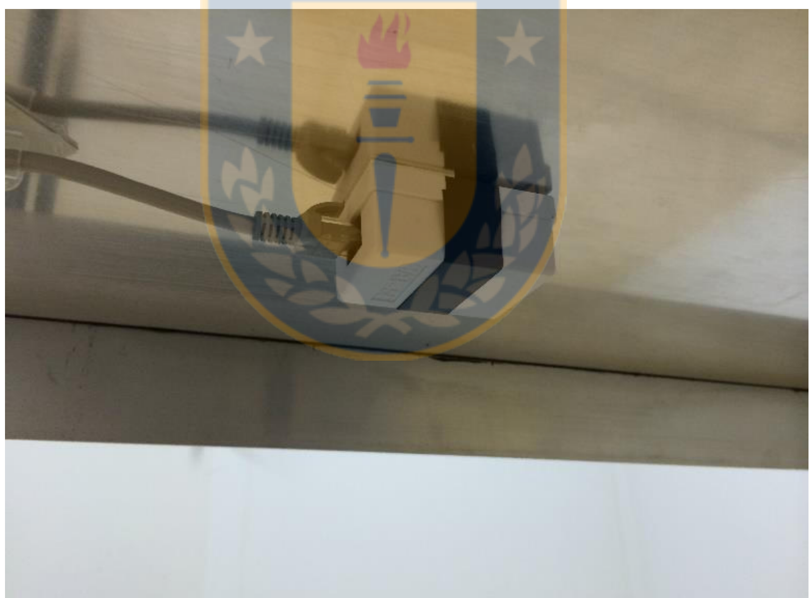

Figure 3.5 Accelerometer placement at middle span.

The chamber is an isolated 20 m^2 room (Figure 3.6), which can be set any temperature, ranging from 0 to 40 °C. The temperature control system includes a three fan system (Figure 3.7). Humidity can also be controlled in the climate chamber, though not addressed in this study.

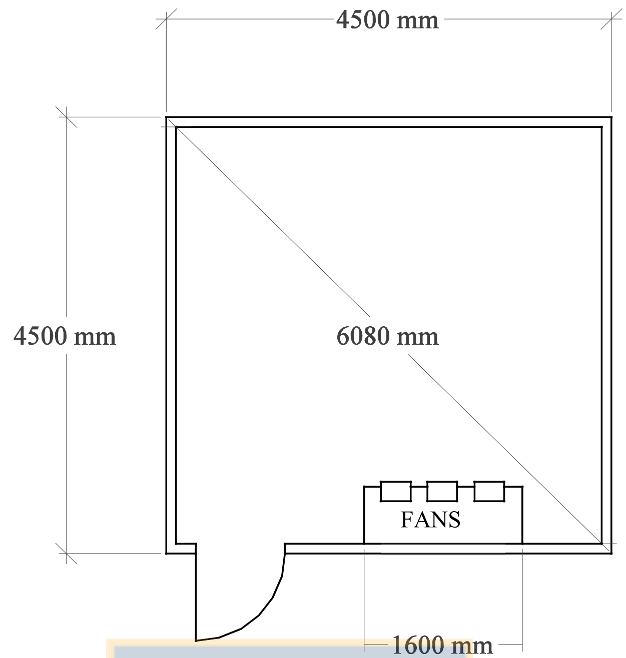

Figure 3.6 Climate chamber dimensions.

Figure 3.7 Uniform temperature distribution application.

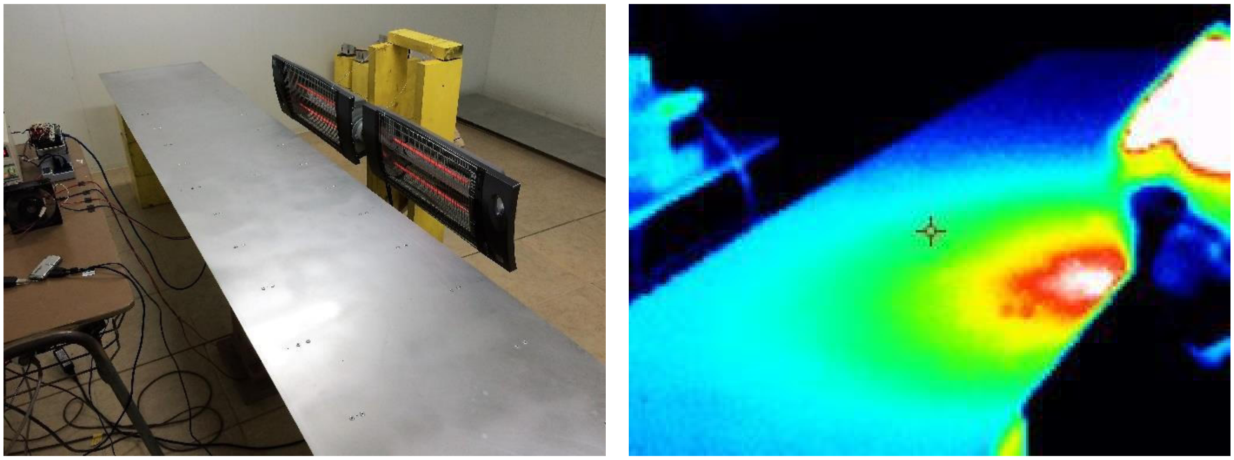

a) Focal Heat system. b) Non-uniform thermal distribution.

Figure 3.8 Non-uniform temperature distribution application.

For non-uniform temperature distribution tests, two heaters are installed, with a 2000 W combined electric power (Figure 3.8a). We use a Fluke Ti20 thermal camera for temperature inspection. A differential of approximately 10 °C is obtained across the deck in all non-uniform temperature distribution tests (Figure 3.8b).

A finite elements model of the structure is created to simulate damage scenarios along the structure. The FEM model is calibrated with laboratory data in terms of the fundamental frequency.

3.3 Finite elements model

A finite elements model, based on the former calibrated finite element model of the structure, is created in order to simulate further temperature scenarios below the freezing point, along the structure. The FEM model is calibrated with laboratory data in terms of the fundamental frequency. All analyses consider temperatures from -5 to 0 °C only.

A material layer is added in top of the deck, which takes into account the behavior of sand (worst case scenario) studied by Simonsen *et al.* (2002), in order to represent a ballast material. As can be seen in Figure 2.10, the resilient modulus of sand has a variation in up to two times the order of magnitude. Therefore, a variation from 100 MPa to 10000 MPa is considered for the study (Table 3.1).

Table 3.1 Material properties under temperature scenarios.

	System temperature (°C)					
Element	**-5**	**-4**	**-3**	**-2**	**-1**	**0**
Deck Layer Elasticity Modulus (MPa)	10000	9800	9290	7970	5090	100
Spring Stiffness (N/m)	2.6×10^8	2.55×10^8	2.42×10^8	2.07×10^8	1.32×10^8	2.6×10^6

To characterize the soil under the effect of temperature, springs are added in each support, as shown in Figure 3.10. Due to the direct relationship between the shear modulus and the stiffness of a spring, an initial value of $2.6\cdot10^6$ (N/m) is taken (Fang, 2013), with an upper limit of $2.6\cdot10^8$ (N/m), as shown in Figure 3.9, thus considering an increase of two orders of magnitude. Calculation of these values are located in Annex 3.1. Table 3.1 shows a summary of values considered for the study. For a simplified analysis, all spring have the same stiffness and no rocking springs are considered.

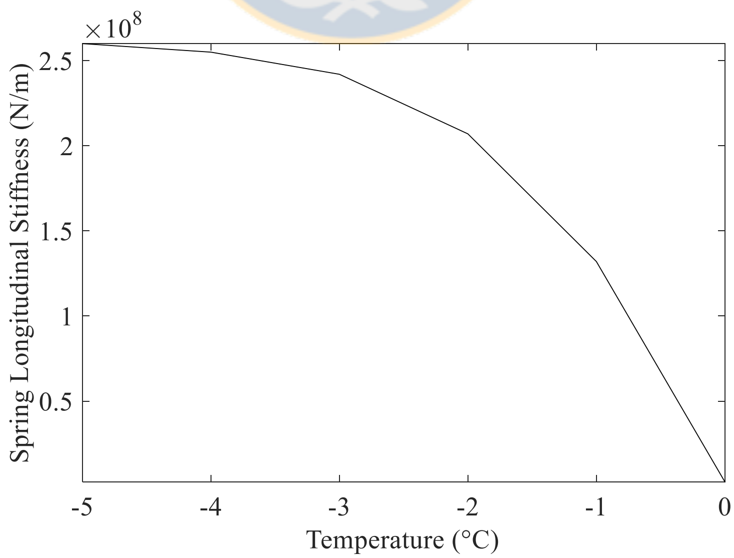

Figure 3.9 Spring longitudinal stiffness versus temperature.

Two torsional springs are also added, one on each end of the structure. These springs are intended only to represent different structural border conditions, from pinned to fixed, not boundary conditions due to temperature scenarios.

Multiple structural configurations are set and data is entered to the finite element software as design points, where spring stiffness, support stiffness and elasticity are the changing variables. An Intel Core i7 computer with 8 cores and 8gb of RAM is used to compute the results. Only the first four vibrational modes are used for the analysis (Figure 3.11). A summary of natural frequencies is shown in Table 3.2.

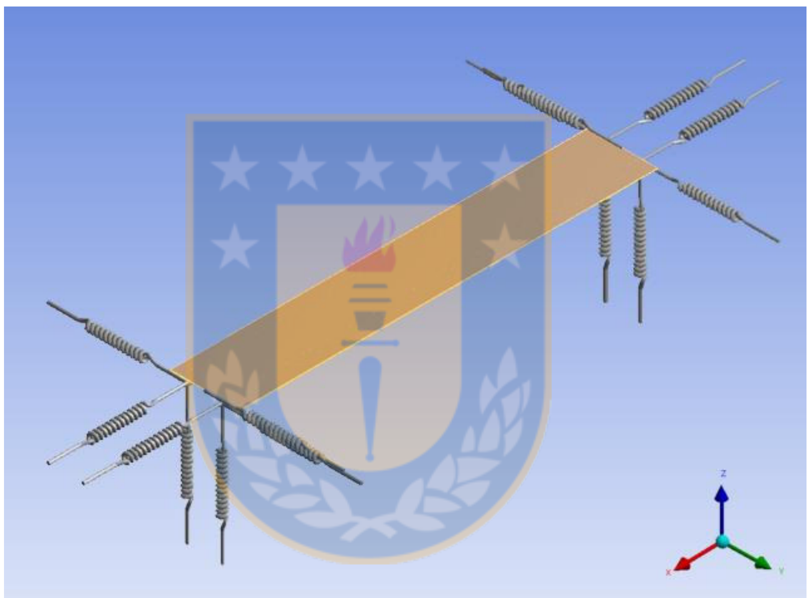

Figure 3.10 Finite elements model.

Table 3.2 Natural frequencies of pinned structure for zero degrees Celsius.

	Vibrational Mode			
	1	**2**	**3**	**4**
Type	Bending	Torsional	Bending	Torsional
Frequency (Hz)	12.21	20.95	39.54	52.25

Figure 3.11 Modal shapes of finite element model.

3.4 Conclusions

A simplified laboratory scaled model and a finite elements model are created. These models allow the testing of damage and temperature scenarios above and below the freezing point. It is expected dynamic properties vary with temperature scenarios, showing in some cases changes greater than the ones produced by damage. Furthermore, soil and deck/ballast are simulated as springs and a second layer over the bridge, which under temperature variations might produce greater changes on dynamic properties than previous results.

SECTION 4 MODEL TESTING

4.1 Introduction

In order to study the effect of temperature over the model, temperature variation, above the freezing point, is induced in laboratory to analyze changes in the dynamic properties of the model. Then, a finite elements model is calibrated with laboratory data to simulate further damage scenarios.

A second finite elements model is later created, based on the former finite element laboratory model, where multiple temperature scenarios below the freezing point and boundaries conditions are considered. The effect of freezing on surrounding soil is simulated as supporting springs with variable stiffness and the effect of deck freezing is simulated as a layer material over the deck with variable elasticity.

For freezing temperature scenarios, variations in frequency are, in certain cases, up to twelve times higher than the ones obtained in temperature ranges above the freezing point. Consequently, the evaluation of freezing temperature effect should be addressed in order to avoid misdiagnosis in bridge monitoring systems.

4.2 Laboratory model testing

A uniform temperature distribution (UTD) in the laboratory structure shows a clear correlation between the fundamental frequency and temperature (Figure 4.1). A total of 0.92% of frequency variation is observed between 0 and 40 °C. Damping does not present any correlation with temperature variation.

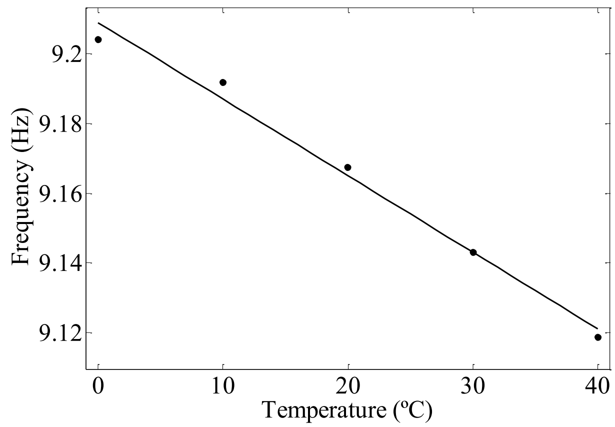

Figure 4.1 Fundamental frequency vs temperature for uniform temperature distribution.

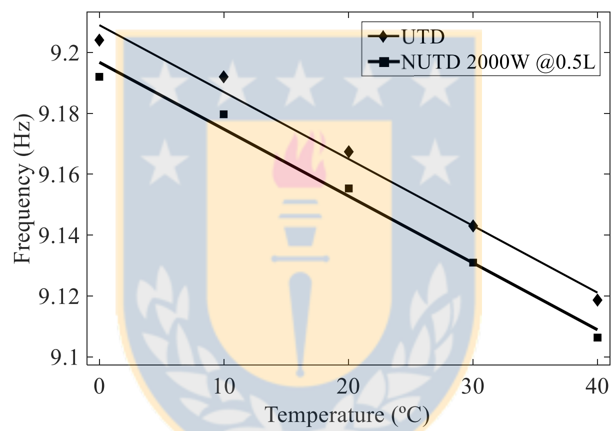

Figure 4.2 Non-uniform and uniform temperature distribution curves comparison.

Non-uniform temperature distribution (NUTD) is tested along with uniform temperature distribution. Tests show the biggest frequency variation is caused by the placement of a heat source at the bridge midspan. When localized heat is applied, curves show a slight fall compared to the uniform distribution test, but maintain a linear relationship between 0 and 40 °C (Figure 4.2). Even though this variation is in the same order as the uniform temperature test, non-uniform temperature distribution is not considered as a relevant parameter to be studied. Only a maximum of 0.13% frequency variation is obtained considering uniform temperature distribution as a baseline Damping is not analyzed as resembles the behavior shown in the uniform distribution test.

Some scenarios associated with a crack in one of the main girders are simulated. To induce damage in the finite elements model, a small cut with different depths at 9 different locations is induced to produce 36 different damage scenarios, where up to a 36% of inertia reduction is obtained in the girder considering a 20 mm cut depth. Finally, if compared with laboratory data, frequency variation produced by certain cases of simulated damage is in the range of variation produced by a uniform temperature distribution (Figure 4.3).

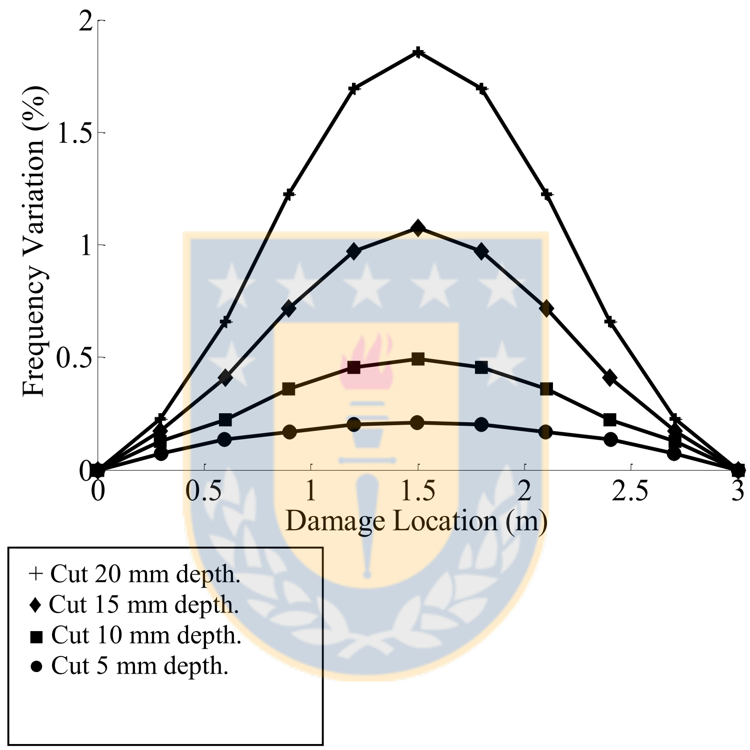

Figure 4.3 Frequency variation considering damage at several locations.

4.3 Finite element model tests results

Frequency variation surfaces are generated for the finite element model under freezing temperature (Figure 4.4). First bending mode presents a high frequency variation for a pinned boundary configuration, with a maximum frequency variation of 12% (Figure 4.5); however, for more constrained boundary conditions, torsional modes present higher frequency variations than the ones observed in bending modes (Figures 4.6 and 4.7).

To understand the contribution of supporting springs or structure under freezing temperatures to the variation of frequency, results are decomposed into two different cases: the first one includes only variations in the deck layer material elasticity, where the second includes mechanical variations only in springs, which simulates soil variations due to freezing temperature. Frequency surface variation tables are found in Annex 4.1.

As can be observed from Figures 4.8 , 4.9 , 4.1 , 4.11, when the layer material is exposed to freezing temperatures, torsional modes are more sensitive to frequency variations than bending modes. Table 4.1 presents the contribution of support springs and layer material to the global variation of frequency, where the latter has bigger variations in torsional modes.

Table 4.1 Maximum frequency variation contribution

	1st Bending Mode			**1st Torsional Mode**			**2nd Bending Mode**			**2nd Torsional Mode**		
Case	**Pinned**	**Semi**	**Fixed**	**Pinned**	**Semi**	**Fixed**	**Pinned**	**Semi**	**Fixed**	**Pinned**	**Semi**	**Fixed**
Layer Material	8.4%	41.0%	**54.6%**	**84.4%**	**77.3%**	**76.1%**	**72.2%**	43.3%	41.9%	**55.5%**	**53.2%**	**52.8%**
Support Springs	**91.6%**	**59.0%**	45.4%	15.6%	22.7%	23.9%	27.8%	**56.7%**	**58.1%**	44.5%	46.8%	47.2%

Previous results showed a global temperature variation from 0 to 40 °C only presents a variation in frequency smaller than 1% (Figure 4.3). Therefore, for freezing temperatures, a variation up to 12 times higher can be found if previous results are compared with Figure 4.5. Furthermore, low damage scenarios were in the order of 2%. These are the orders of magnitude of change in the natural frequencies: 1% for uniform temperature 0°C-40°C, 12% below freezing temperature, and 2% for damage scenarios. These results stress the need for further studying damage sensitive features and the need for data normalization for SHM applications.

Frequency surfaces can be transformed later into normalization surfaces by subtracting percentage results to 100%.

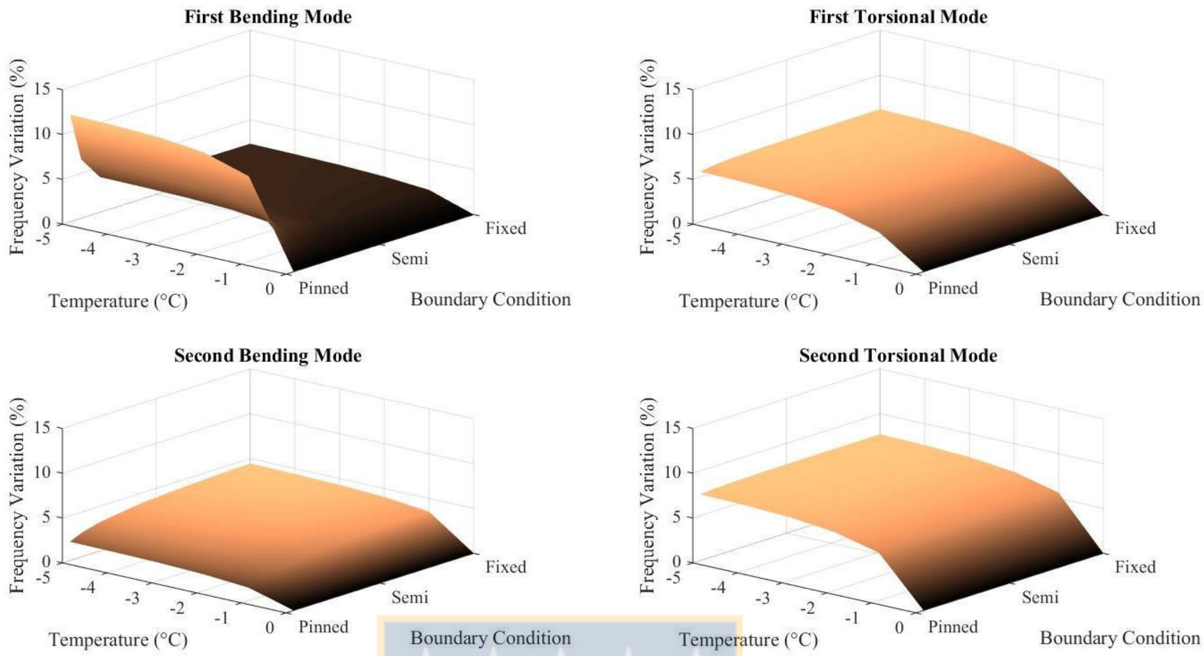

Figure 4.4 Frequency variation surfaces for finite elements model under freezing temperature.

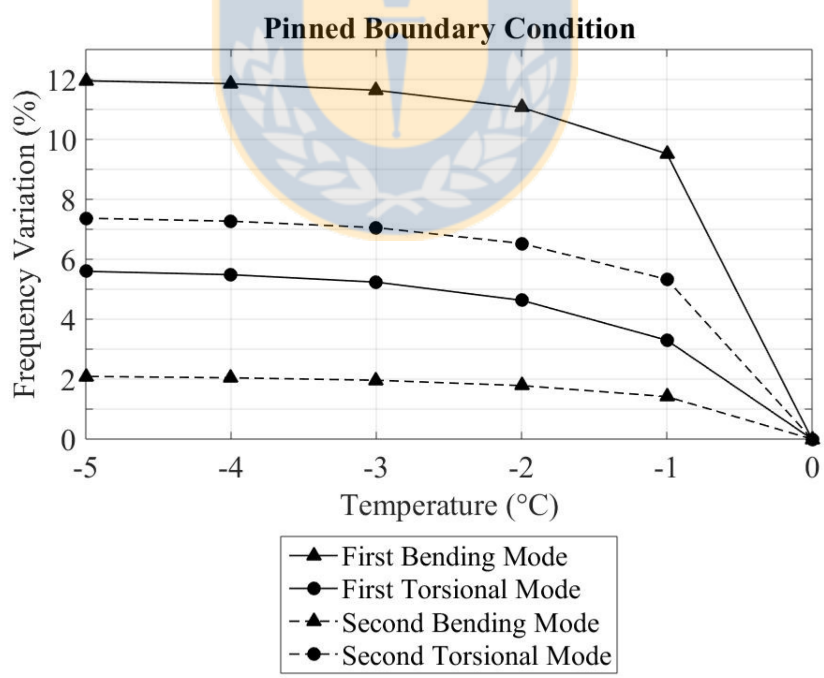

Figure 4.5 Frequency variation in finite elements model under freezing temperature for pinned boundary condition.

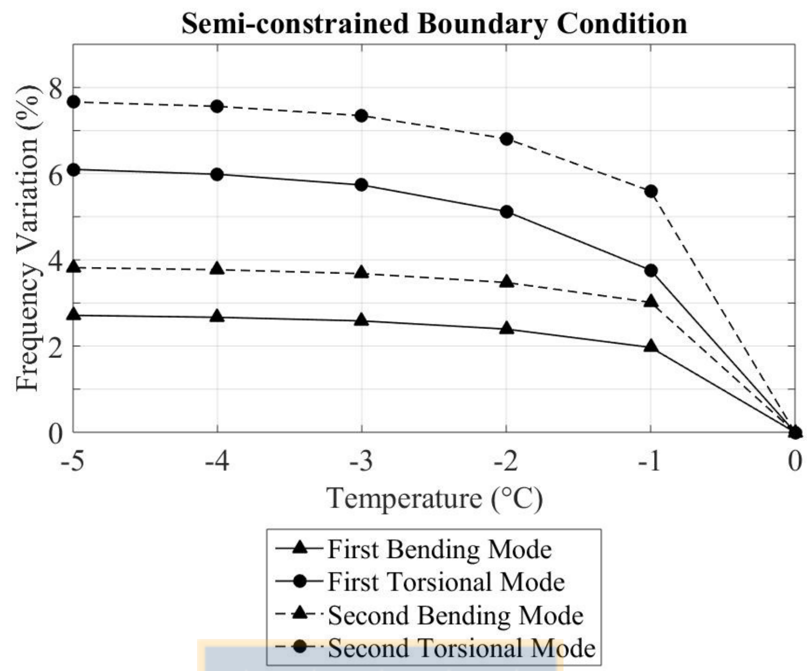

Figure 4.6 Frequency variation in finite elements model under freezing temperature for semi-constrained boundary condition.

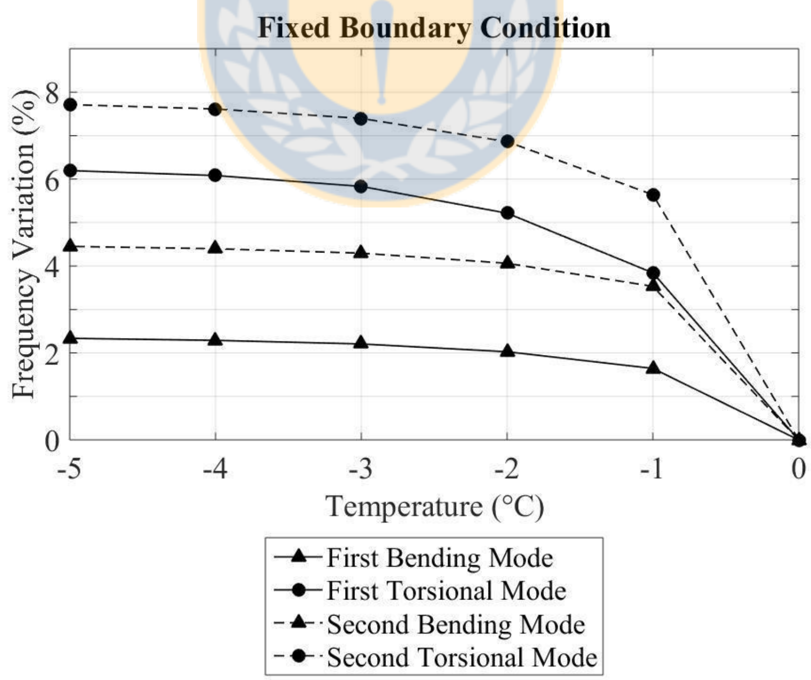

Figure 4.7 Frequency variation in finite elements model under freezing temperature for fixed boundary condition.

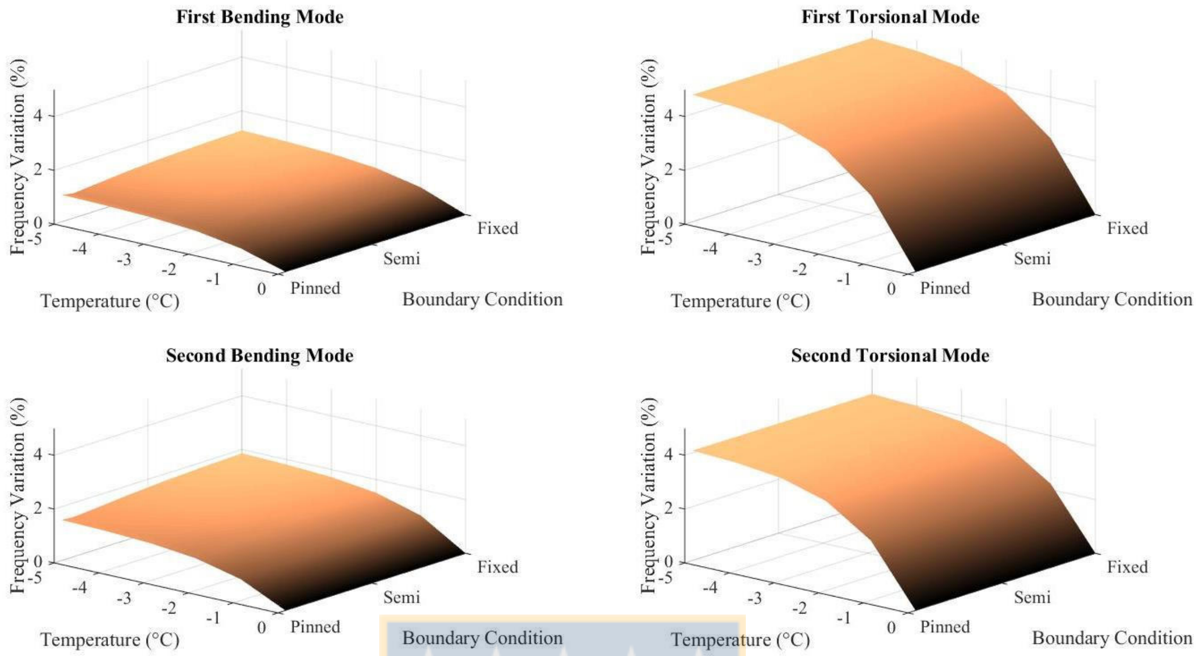

Figure 4.8 Frequency variation contribution of layer material under freezing temperature.

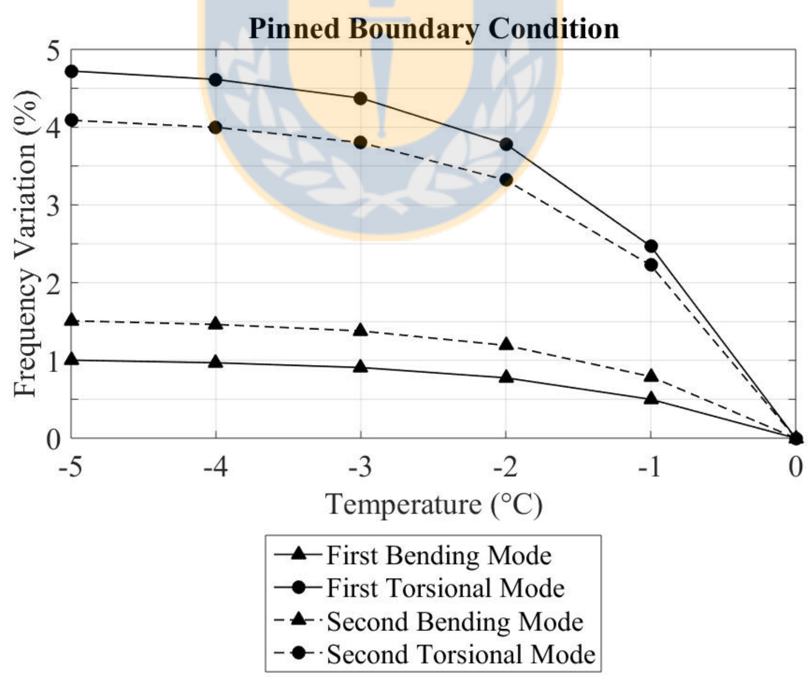

Figure 4.9 Frequency variation contribution of layer material under freezing temperature for pinned boundary condition.

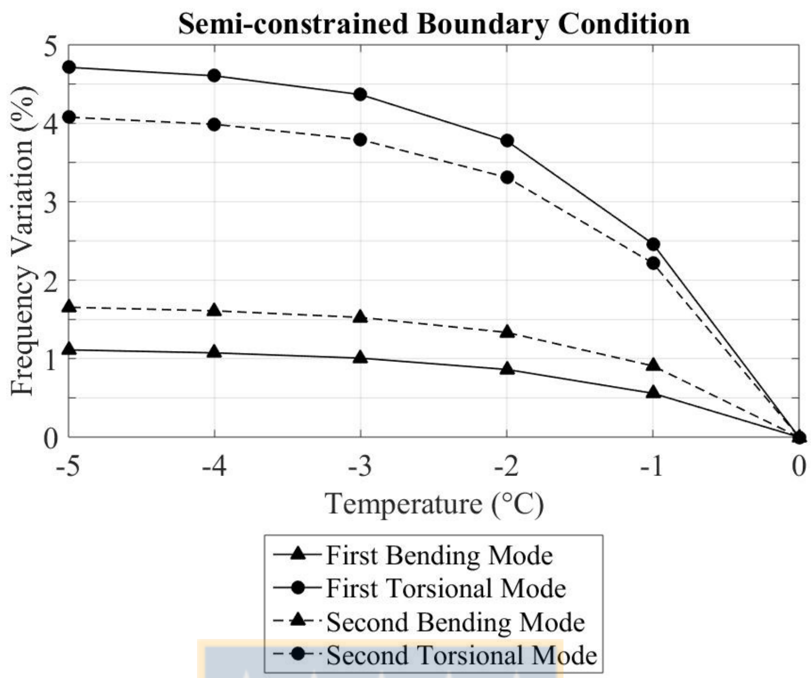

Figure 4.10 Frequency variation contribution of layer material under freezing temperature for semi-constrained boundary condition.

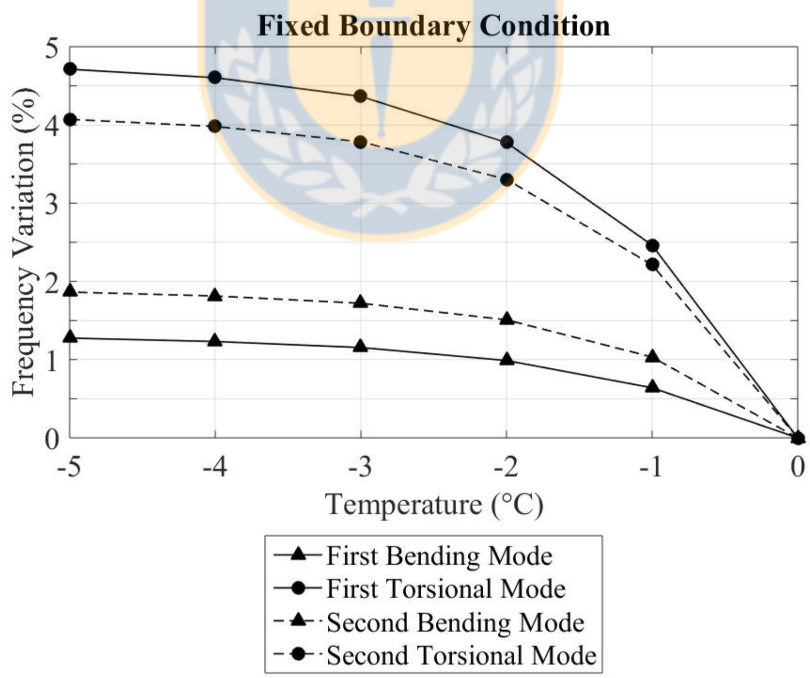

Figure 4.11 Frequency variation contribution of layer material under freezing temperature for fixed boundary condition.

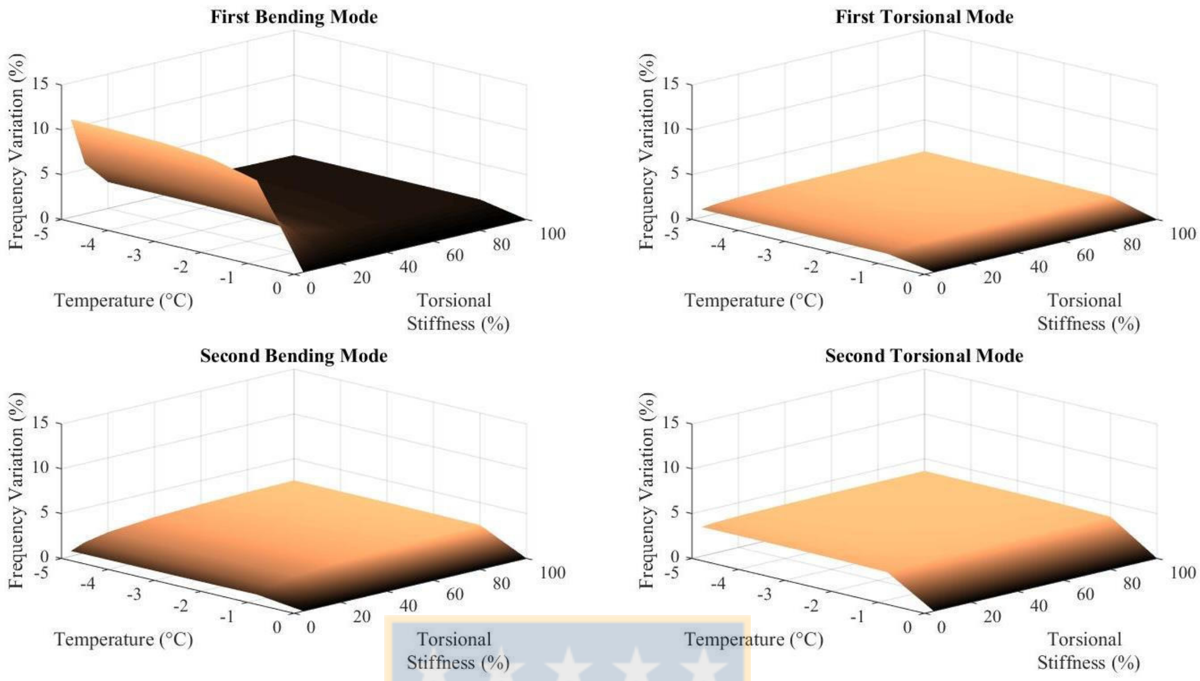

Figure 4.12 Frequency variation contribution of supporting springs under freezing temperature.

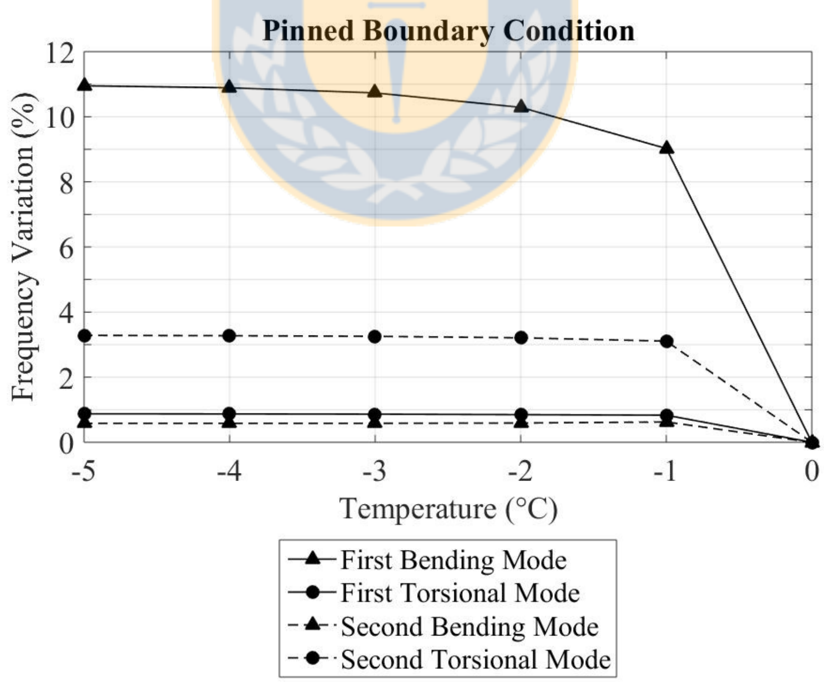

Figure 4.13 Frequency variation contribution of supporting springs under freezing temperature for pinned boundary condition.

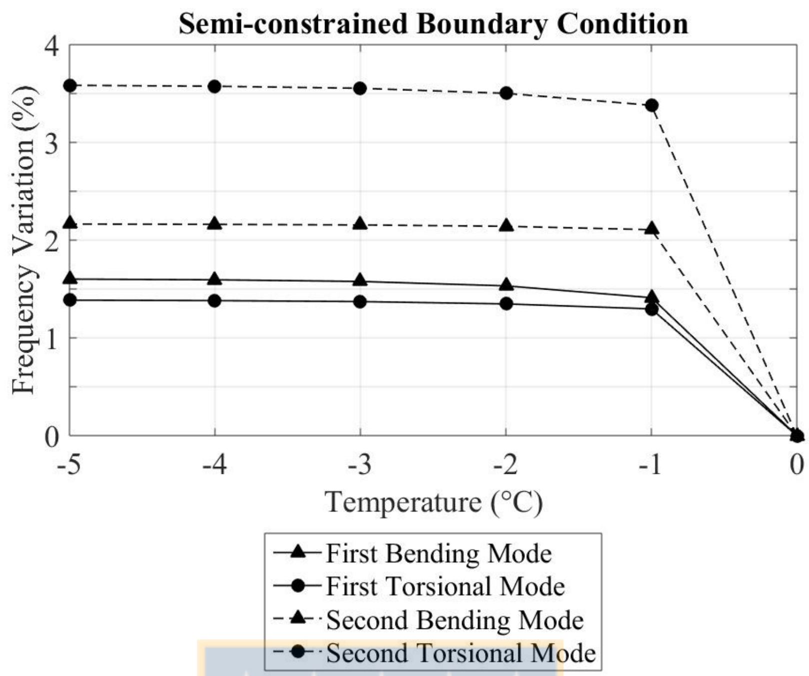

Figure 4.14 Frequency variation contribution of supporting springs under freezing temperature for semi-constrained boundary condition.

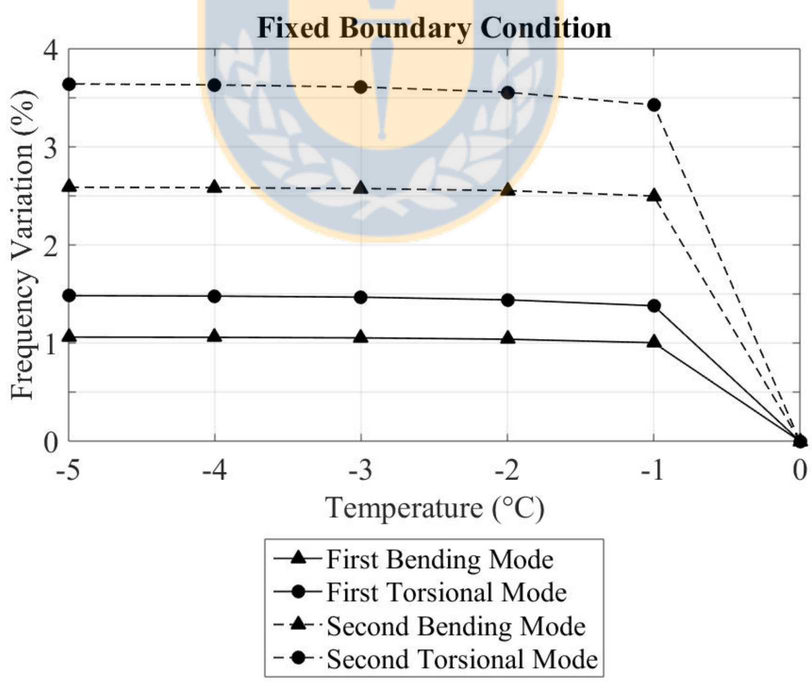

Figure 4.15 Frequency variation contribution of supporting springs under freezing temperature for fixed boundary condition.

4.4 Proposed data normalization method

In structural health monitoring systems, data normalization is required in order to study changes in dynamic parameters, where long time monitoring windows are needed to understand the behavior of the structure under several environmental conditions. However, to avoid misdiagnosis at early stages, prior knowledge of these conditions is needed before the SHM system is fully functional.

As can be concluded from Table 4.1, torsional modes are significantly influenced by variations in the surface deck than variations in simulated soil. Variations on the simulated soil show a more significant effect on bending vibrational modes than torsional modes. A simple data normalization procedure is outlined for this study:

I. Obtain natural frequencies of the structure through a FEM model analysis.

II. Detect bending and torsional frequencies in the FEM model.

III. Analyze elastic soil behavior under freezing temperature conditions and use it as an input for the FEM model.

IV. Normalize bending vibrational frequencies based on the normalization curves generated.

As an example, Figure 4.13 shows frequency normalization coefficient surfaces, where any frequency value ranging from -5 °C to 0 °C, from pinned to a fixed boundary condition is multiplied by a coefficient which normalizes it. For this study, this normalization surface could be integrated in structural health monitoring algorithms to minimize the temperature effect due to thermal variations in bending modes.

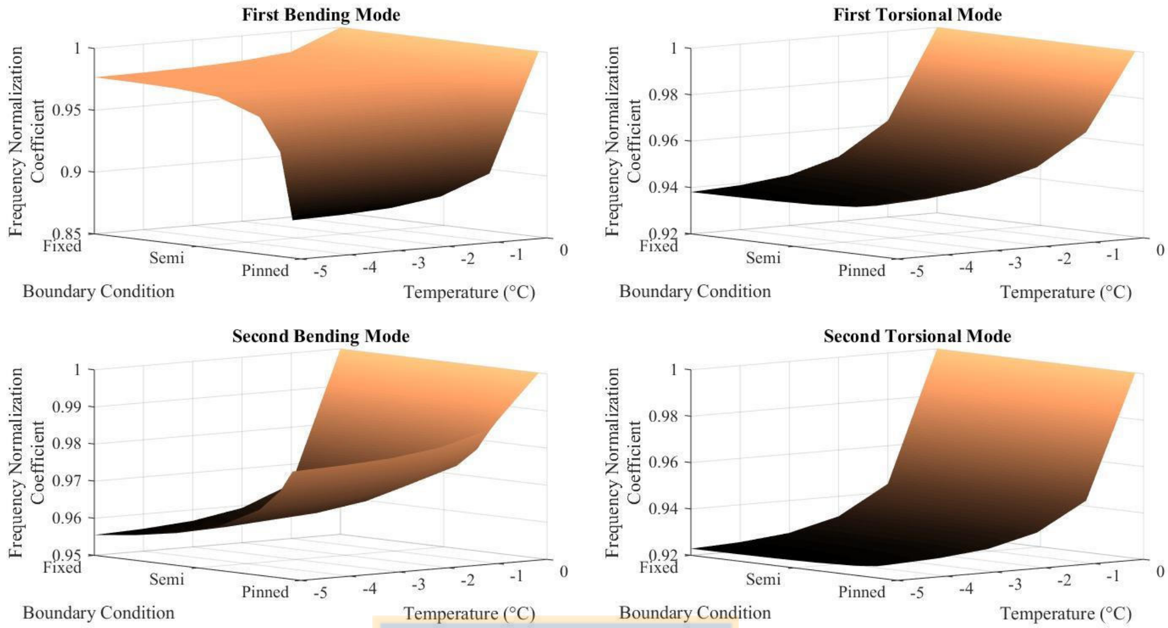

Figure 4.16 Frequency normalization surfaces.

4.5 Conclusions

A practical method for studying the effect of freezing temperatures in bridge structures is applied. Variation of material and support conditions due to low temperature scenarios are included into a finite elements bridge model.

For a mildly rigid structure under freezing scenarios, results show a direct relationship between surface deck variations and frequency variations in torsional modes, where variations in bending modes are related to supporting springs changes due to low temperatures. For a more rigid structure, the contribution of frequency variation due to changes in the surface deck is diminished by greater frequency variations caused by changes in supports due to freezing temperatures.

High frequency variations may not only be expected in railway bridges, but also in every bridge structure under extreme low temperature environments. Further research in real case structures is needed in order to have a better understanding of the problem.

Even though the contribution of the frozen layer material to the global variation of frequency is high for the studied laboratory scale model, its contribution is unknown for real case scenarios, full scale structures with a bigger complexity in terms of structural configuration.

SECTION 5 CONCLUSIONS

A study on the effect of low temperature on a finite elements model based on a laboratory scaled bridge has been performed. A deck layer material and springs are added to the system in order to simulate the effect of ballast and soil, respectively, under the effect of freezing temperature scenarios.

In some scenarios, springs contribution -due to freezing temperature- on the frequency variation of the system is observed to be greater than the frequency variation produced by changes in the deck surface. This implies that variations in frequency of complex bridge structures could be produced mainly by the surrounding soil under low temperature conditions, instead of variations in mechanical properties of asphalt or ballast on railway bridges. Even though it is good assumption, due to the possible low contribution of rigidity of ballast or asphalt to the global rigidity of a structure, further research is needed before being able to extend it to real case scenarios.

Not considering variations due to freezing temperature conditions could lead to critical misdiagnosis in structural health monitoring systems. Furthermore, long monitoring periods are needed in order to address all environmental conditions bridge structures in extreme environments face during operation. However, unlike iterative methods, which use data from instrumented structures, in this research a more practical monitoring approach is taken. This approach allows to understand the behavior of the structure before the monitoring system is implemented, and can only be accomplished by studying the mechanical behavior of materials under environmental conditions. Therefore, monitoring of the surrounding soil of bridge is recommended, before and during a bridge structural health monitoring program.

Complex bridge structures under temperature scenarios must be studied, where dynamic variations could be produced mainly by the surrounding soil under low temperature conditions, instead of variations in mechanical properties of asphalt or ballast on railway bridges. Even though it is good assumption, due to the possible low rigidity contribution of the surface to the global rigidity of a structure, further research has to be pursued along these lines.

SECTION 6 REFERENCES

Cornwell, P.J, C.R. Farrar, S.W. Doebling and H. Sohn (1999) Environmental variability of modal properties. **Experimental Techniques 23(6)**. 45-48.

Doebling, S. W., and C. R. Farrar (1997). Using statistical analysis to enhance modal-based damage identification. **Structural Damage Assessment Using Advanced Signal Processing Procedures**: 199-210.

Fang, H. Y. (2013). **Foundation engineering handbook**. Springer Science & Business Media. Berlin.

Farrar, C. R., W.E. Baker, T.M. Bell, K.M. Cone, T.W. Darling, T.A. Duffey, and A. Migliori (1994). Dynamic characterization and damage detection in the I-40 bridge over the Rio Grande. **Los Alamos National Laboratory**, New Mexico.

Fu, Yongda, and J.T. DeWolf (2001) Monitoring and analysis of a bridge with partially restrained bearings. **Journal of Bridge Engineering 6.1**. 23-29.

Guzman, N. (2015) **Estudio de la temperatura global y gradientes térmicos en el comportamiento dinámico de un modelo simplificado de puente en laboratorio**. Undergraduate Thesis. Departamento de Ingeniería Civil. Universidad de Concepción. Concepción.

Gonzales, I., M. Ülker-Kaustell, and R. Karoumi (2013). Seasonal effects on the stiffness properties of a ballasted railway bridge. **Engineering structures**, **57.** 63-72.

Kim, J. T., J.H. Park and B.J. Lee (2007) Vibration-based damage monitoring in model plate-girder bridges under uncertain temperature conditions. **Engineering Structures, 29(7)**. 1354-1365.

Peeters B., and G. DeRoeck (2001) One-year monitoring of the Z 24-Bridge: environmental effects versus damage events. **Earthquake engineering & structural dynamics 30.2.** 149-171.

Simonsen K., V.C. Janoo, and U. Isacsson (2002) Resilient properties of unbound road materials during seasonal frost conditions. **Journal of Cold Regions Engineering 16.1**. 28-50.

Sohn, H., M. Dzwonczyk, E.G Straser, A.S Kiremidjian, K.H Law and T. Meng (1999). An experimental study of temperature effect on modal parameters of the Alamosa Canyon Bridge. **Earthquake Engineering & Structural Dynamics, 28**. 879–897.

Sohn, H. (2007). Effects of environmental and operational variability on structural health monitoring. **Philosophical Transactions of the Royal Society of London A: Mathematical, Physical and Engineering Sciences, 365(1851),** 539-560.

Xia, Y., B. Chen, S. Weng, Y. Ni, Y. Q. y Y. L. Xu (2012) Temperature effect on vibration properties of civil structures: A literature review and case studies. **Journal of Civil Structural Health Monitoring, 2.** 29-46

Zabel V., B. Maik and N. Susanne (2010). The influence of temperature varying material parameters on the dynamic behavior of short span railway bridges. **Proc. International Conference on Noise and Vibration Engineering (ISMA), 74**. Leuven, Belgium.

ANNEX 3.1 SPRING STIFFNESS CALCULATION

In order to calculate the supporting springs stiffness, a squared 1cm^2 contact area is considered. According to Fang (2013), the stiffness of a spring associated with a foundation is calculated as follows:

Vertical, Z:

$$K_Z = \frac{4.54GB}{1-v} \quad \text{(A3.1.1)}$$

Horizontal, X and Y

$$K_X = K_Y = \frac{9GB}{2-v} \quad \text{(A3.1.2)}$$

Where G: Shear Modulus, B: Length of Base, *v*: Poisson Ratio. Finally,

$$G = \frac{E}{2(1+v)} = \frac{100}{2(1+0.33)} = 37.6\,\text{MPa} \quad \text{(A3.1.3)}$$

$$K_Z = \frac{4.54GB}{1-v} = \frac{4.54 \cdot 37.6e6 \cdot 0.01}{1-0.33} = 2.6 \cdot 10^6\,\text{N/m} \quad \text{(A3.1.4)}$$

$$K_X = K_Y = \frac{9 \cdot 37.6e6 \cdot 0.01}{2-0.33} = 2.0 \cdot 10^6\,\text{N/m} \quad \text{(A3.1.5)}$$

To simplify the analysis and as both horizontal and vertical springs values are in the same order of magnitude, *Kz* is chosen as the value for all springs.

ANNEX 4.1 FREQUENCY VARIATION FOR FINITE ELEMENTS MODEL

Table A.1.1 Frequency percentage variation, 1st mode. Springs and layer material considered.

MODE 1	**Frequency variation (%)**					
Tors. Stiffness (%)	**0 °C**	**-1 °C**	**-2 °C**	**-3 °C**	**-4 °C**	**-5 °C**
4	0	9.524576	11.0652	11.64081	11.85854	11.9552
10	0	5.108737	6.002517	6.351961	6.489792	6.554615
20	0	2.966378	3.539375	3.778019	3.877661	3.928037
40	0	1.969657	2.394081	2.583634	2.667545	2.712917
60	0	1.741223	2.134269	2.314849	2.396604	2.44189
80	0	1.668791	2.053813	2.232975	2.314902	2.360761
100	0	1.64381	2.027487	2.207187	2.289772	2.336244

Table A.1.2 Frequency percentage variation, 2nd mode. Springs and layer material considered.

MODE 2	**Frequency variation (%)**					
Tors. Stiffness (%)	**0 °C**	**-1 °C**	**-2 °C**	**-3 °C**	**-4 °C**	**-5 °C**
4	0	3.300495	4.632225	5.238126	5.48515	5.597454
10	0	3.506347	4.847433	5.455008	5.702325	5.814651
20	0	3.652191	5.004536	5.615046	5.863212	5.97581
40	0	3.760088	5.123106	5.736716	5.985849	6.098793
60	0	3.804049	5.171978	5.787075	6.036685	6.149804
80	0	3.827893	5.198624	5.814584	6.064478	6.177701
100	0	3.842861	5.215392	5.831915	6.081986	6.195277

Table A.1.3 Frequency percentage variation, 3rd mode. Springs and layer material considered.

MODE 3	**Frequency variation (%)**					
Tors. Stiffness (%)	**0 °C**	**-1 °C**	**-2 °C**	**-3 °C**	**-4 °C**	**-5 °C**
4	0	1.417061	1.78515	1.962523	2.044716	2.091042
10	0	1.983886	2.363414	2.539912	2.620012	2.664301
20	0	2.503612	2.914808	3.100968	3.183995	3.229128
40	0	3.014197	3.475526	3.680596	3.770917	3.819389
60	0	3.270941	3.764339	3.982227	4.077753	4.128772
80	0	3.426364	3.941343	4.168006	4.267149	4.319969
100	0	3.532523	4.062977	4.295968	4.397732	4.451869

Table A.1.4 Frequency percentage variation, 4th mode. Springs and layer material considered.

MODE 4	**Frequency variation (%)**					
Tors. Stiffness (%)	**0 °C**	**-1 °C**	**-2 °C**	**-3 °C**	**-4 °C**	**-5 °C**
4	0	5.330966	6.527928	7.055911	7.271404	7.371567
10	0	5.449065	6.651328	7.180293	7.395965	7.49614
20	0	5.533824	6.742653	7.27337	7.489555	7.589897
40	0	5.596801	6.811885	7.344446	7.561213	7.661763
60	0	5.622204	6.840118	7.373547	7.590594	7.691247
80	0	5.635238	6.854674	7.388577	7.60578	7.706489
100	0	5.641039	6.861297	7.395462	7.612748	7.713489

Table A.1.5 Frequency percentage variation, 1st mode. Only variation in layer material considered.

MODE 1	Frequency variation (%)					
Tors. Stiffness (%)	**0 °C**	**-1 °C**	**-2 °C**	**-3 °C**	**-4 °C**	**-5 °C**
4	0	0.499771	0.776273	0.90838	0.969443	1.003774
10	0	0.460133	0.712284	0.832487	0.888209	0.919656
20	0	0.492894	0.761434	0.889312	0.94863	0.982274
40	0	0.558311	0.861874	1.006398	1.073517	1.111632
60	0	0.597899	0.922962	1.077755	1.149653	1.190525
80	0	0.623135	0.961982	1.123355	1.19833	1.240963
100	0	0.640472	0.98879	1.154705	1.231805	1.275642

Table A.1.6 Frequency percentage variation, 2nd mode. Only variation in layer material considered.

MODE 2	Frequency variation (%)					
Tors. Stiffness (%)	**0 °C**	**-1 °C**	**-2 °C**	**-3 °C**	**-4 °C**	**-5 °C**
4	0	2.468506	3.783253	4.374132	4.613798	4.722385
10	0	2.465739	3.77907	4.369307	4.608728	4.717179
20	0	2.464331	3.776941	4.366866	4.606139	4.714543
40	0	2.463481	3.775663	4.365392	4.604599	4.712955
60	0	2.463167	3.775189	4.364847	4.604014	4.71237
80	0	2.462995	3.774939	4.36455	4.603707	4.712058
100	0	2.46289	3.774771	4.364361	4.603514	4.711857

Table A.1.7 Frequency percentage variation, 3rd mode. Only variation in layer material considered.

MODE 3	**Frequency variation (%)**					
Tors. Stiffness (%)	**0 °C**	**-1 °C**	**-2 °C**	**-3 °C**	**-4 °C**	**-5 °C**
4	0	0.792253	1.193397	1.378829	1.462772	1.509154
10	0	0.787104	1.175142	1.352461	1.431962	1.475412
20	0	0.826361	1.223675	1.403315	1.483154	1.526368
40	0	0.907218	1.33395	1.525215	1.609637	1.654978
60	0	0.963401	1.412071	1.612445	1.700648	1.747878
80	0	1.002805	1.466996	1.673885	1.764826	1.813444
100	0	1.033287	1.50898	1.72069	1.813662	1.863316

Table A.1.8 Frequency percentage variation, 4th mode. Only variation in layer material considered.

MODE 4	**Frequency variation (%)**					
Tors. Stiffness (%)	**0 °C**	**-1 °C**	**-2 °C**	**-3 °C**	**-4 °C**	**-5 °C**
4	0	2.223835	3.319114	3.801207	3.9975	4.088451
10	0	2.220382	3.314235	3.795747	3.991815	4.082665
20	0	2.218502	3.311596	3.792802	3.988751	4.079552
40	0	2.217181	3.309765	3.790769	3.986643	4.077411
60	0	2.216379	3.3087	3.789605	3.985441	4.076195
80	0	2.215286	3.307344	3.788157	3.983962	4.074703
100	0	2.212483	3.304123	3.784812	3.980574	4.071299

Table A.1.9 Frequency percentage variation, 1st mode. Only variation in springs considered.

MODE 1	**Frequency variation (%)**					
Tors. Stiffness (%)	**0 °C**	**-1 °C**	**-2 °C**	**-3 °C**	**-4 °C**	**-5 °C**
4	0	9.024804	10.28892	10.73242	10.8891	10.95143
10	0	4.648604	5.290233	5.519474	5.601582	5.634958
20	0	2.473484	2.77794	2.888708	2.92903	2.945763
40	0	1.411346	1.532207	1.577235	1.594028	1.601286
60	0	1.143324	1.211307	1.237094	1.246951	1.251365
80	0	1.045656	1.091831	1.10962	1.116572	1.119798
100	0	1.003338	1.038697	1.052482	1.057968	1.060602

Table A.1.10 Frequency percentage variation, 2nd mode. Only variation in springs considered.

MODE 2	**Frequency variation (%)**					
Tors. Stiffness (%)	**0 °C**	**-1 °C**	**-2 °C**	**-3 °C**	**-4 °C**	**-5 °C**
4	0	0.831989	0.848972	0.863994	0.871351	0.875068
10	0	1.040608	1.068363	1.085701	1.093596	1.097472
20	0	1.18786	1.227595	1.24818	1.257072	1.261267
40	0	1.296607	1.347444	1.371324	1.381251	1.385838
60	0	1.340882	1.396789	1.422227	1.432671	1.437434
80	0	1.364898	1.423685	1.450034	1.46077	1.465643
100	0	1.379971	1.44062	1.467554	1.478473	1.483421

Table A.1.11 Frequency percentage variation, 3rd mode. Only variation in springs considered.

MODE 3	Frequency variation (%)					
Tors. Stiffness (%)	**0 °C**	**-1 °C**	**-2 °C**	**-3 °C**	**-4 °C**	**-5 °C**
4	0	0.624807	0.591753	0.583694	0.581944	0.581888
10	0	1.196782	1.188272	1.187451	1.18805	1.188888
20	0	1.677252	1.691133	1.697653	1.700841	1.70276
40	0	2.106979	2.141576	2.155382	2.16128	2.164412
60	0	2.30754	2.352268	2.369783	2.377105	2.380894
80	0	2.423559	2.474347	2.494121	2.502323	2.506525
100	0	2.499236	2.553997	2.575278	2.584071	2.588553

Table A.1.12 Frequency percentage variation, 4th mode. Only variation in springs considered.

MODE 4	Frequency variation (%)					
Tors. Stiffness (%)	**0 °C**	**-1 °C**	**-2 °C**	**-3 °C**	**-4 °C**	**-5 °C**
4	0	3.107131	3.208814	3.254705	3.273905	3.283116
10	0	3.228684	3.337093	3.384547	3.40415	3.413475
20	0	3.315321	3.431057	3.480568	3.500804	3.510345
40	0	3.379619	3.50212	3.553677	3.57457	3.584352
60	0	3.405825	3.531418	3.583942	3.605153	3.615052
80	0	3.419952	3.54733	3.60042	3.621818	3.631786
100	0	3.428555	3.557174	3.61065	3.632174	3.64219

ANNEX 4.2 DATA PROCESSING ALGORITHM

```
clc
clear all %#ok<*CLSCR>
close all

% DATA REQUEST
dataExt = 'csv';

% SELECT FOLDER TO READ CSV FILE - LIST ONLY FILES WITH
dataExt EXTENSION
[file,folder] = uigetfile( ...
{'*.csv',...
 'CSV Files (*.csv)';
   '*.*',  'All Files (*.*)'}, ...
   'SELECT FILE');

fileLocation = strcat(folder,file);
mData = csvread(fileLocation,7,15);

% MATRIX CREATION
tempSimulations = 6; % TEMPERATURE SIMULATIONS
nModes = 4; % NUMBER OF MODES

% STIFFNESS SIMULATIONS
vectorStiffSimulations = [200 500 1000 2000 3000 4000
5000];
vectorStiffSimulations = (vectorStiffSimulations ./
max(vectorStiffSimulations))*100;
stiffSimulations = length(vectorStiffSimulations);
mTorsionalStiff =
repmat(vectorStiffSimulations,tempSimulations,1)';

vTemperature = [0 -1 -2 -3 -4 -5]; % TEMPERATURE TESTS
mTemperature = zeros(stiffSimulations,tempSimulations);
% TEMPERATURE MATRIX
mFrequency = zeros(stiffSimulations,tempSimulations,
nModes); % FREQUENCY MATRIX
mFrequencyFixed =
zeros(stiffSimulations,tempSimulations, nModes); %
FREQUENCY MATRIX FIXED
```

```
tCounter = 0; % TEMPERATURE MATRIX CREATION
for i = 1: tempSimulations
   for j = 1 : stiffSimulations
        tCounter = tCounter + 1;
        mTemperature(j,i) = mData(tCounter,1);
   end
end

for k = 2 : nModes + 1 % FREQUENCY MATRIX CREATION
    tCounter = 0;
    for i = 1: tempSimulations
       for j = 1 : stiffSimulations
            tCounter = tCounter + 1;
            mFrequency(j,i,k-1) = mData(tCounter,k);
       end
    end
end

for k = 2 : nModes + 1 % FREQUENCY FIXED MATRIX
CREATION
    for i = 1: stiffSimulations
       for j = 1 : tempSimulations
           mFrequencyFixed(i,j,k-1) =
((mFrequency(i,j,k-1)/mFrequency(i,1,k-1))-1)*100;
           %mFrequencyFixed(i,j,k-1) =
((mFrequency(i,j,k-1)/mFrequency(1,1,k-1))-1)*100;
       end
    end
end

% PLOTTING
figure
box on
grid off
plotOrder = [1 2 3 4];
plotNames = {'First Bending Mode' 'First Torsional
Mode' 'Second Bending Mode' 'Second Torsional Mode'};

fontS = 12;
fontN = 'Times';
figureHandle = gcf;
```

```
set(findall(figureHandle,'type','figure'),'color','w','
Position',[200 200 1200 800])
set(findall(figureHandle,'type','text'),'fontSize',font
S,'fontName',fontN)

for i = 1 : nModes
    subplot(2,2,plotOrder(i))
    [xq,yq] = meshgrid(-5:0.05:0, -0.2:0.05:100);
    %vq =
griddata(mTemperature,mTorsionalStiff,mFrequencyFixed(:
,:,i),xq,yq);
    vq =
interp2(mTemperature,mTorsionalStiff,mFrequencyFixed(:,
:,i),xq,yq);

    h = surf(xq,yq,vq);
    %light('Position',[0 0 50])
    shading interp;
    colormap copper;
    view([45,30]);

    title(plotNames(plotOrder(i)));
    xlabel('Temperature (°C)');
    ylabel({'  Torsional';'Stiffness (%)'});
    zlabel('Frequency Variation (%)');

    xlim([min(vTemperature) 0]);
    ylim([0 100]);

    vTop = ceil(max(max(max(mFrequencyFixed(:,:,:)))));
    zlim([0 round2(vTop,5) ]);
    axisHandle = gca;
    set(axisHandle,'fontname',fontN,'fontSize',fontS);
    axisHandle.YTick = [0 20 40 60 80 100];
end
```